

Important declarations

Please remove this info from manuscript text if it is also present there.

Associated Data

Data supplied by the author:

The raw data will be available as a supplementary Excel file.

Required Statements

Competing Interest statement:

The authors declare that they have no competing interests.

Funding statement:

The authors received no funding for this work.

Uneven demographic consequences of the 2022 disease outbreak for the sea urchin *Diadema antillarum* in Puerto Rico

Ruber Rodríguez-Barreras^{Corresp. 1}, Claudia Patricia Ruiz-Díaz², Marcos A. Quiñones-Otero³, Carlos Toledo-Hernández^{Corresp. 2}

¹ Department of Biology, University of Puerto Rico, Mayagüez campus, Call BOX 9000, Mayagüez 00681-9000, Puerto Rico, USA

² Sociedad Ambiente Marino, PO Box 22158, San Juan, Puerto Rico 00931-2158, USA

³ University of Puerto Rico, Río Piedras campus, Planning Department, 10 Ave. Universidad STE 1001, San Juan 00931-2458, Puerto Rico, USA

Corresponding Authors: Ruber Rodríguez-Barreras, Carlos Toledo-Hernández

Email address: ruber.rodriguez@upr.edu, carlostoledo@sampr.org

Pervasive epizootic events have had a significant impact on marine invertebrates throughout the Caribbean, leading to severe population declines and consequential ecological implications. One such event was the regional collapse of herbivory, partly caused by the *Diadema antillarum* mortality event in 1983-84, resulting in a trophic cascade and altering the structure of reef communities. Consequently, there was a notable decrease in coral recruitment and an increase in the coverage of macroalgae. Nearly four decades later, in early 2022, the Caribbean basin experienced another widespread mass mortality event, further reducing the populations of *D. antillarum*. To assess the effects of this recent mortality event on the current demographics of *D. antillarum*, we surveyed eight populations along the eastern, northeastern, northern, and northwestern coast of Puerto Rico from May to July 2022, estimating their population density, size distribution, and disease prevalence. Additionally, the study compared these population parameters with data from four sites previously surveyed in 2012 and 2017 to understand the impact of the recent mortality event. The survey conducted in 2022 showed varying population densities at the surveyed reefs. Some populations exhibited mean densities of nearly one individual per square meter, while others had extremely low or no living individuals per square meter. The four populations with the highest density showed no evidence of disease, whereas the four populations with the lowest *D. antillarum* densities exhibited moderate to high disease prevalence. However, when considering all sites, the estimated disease prevalence remained below 5%. Nevertheless, the comparison with data from 2012 and 2017 indicated that the recent mortality event had a negative impact on *D. antillarum* demographics at multiple sites, as the densities in 2022 were reduced by 60.19% compared to those from the previous years. However, it is still too early to determine the severity of this new mortality event compared to the 1983-84 mortality

event. Therefore, it is imperative to continue monitoring these populations.

1 **Uneven demographic consequences of the 2022 disease outbreak for the sea**
2 **urchin *Diadema antillarum* in Puerto Rico**

3 Ruber Rodríguez-Barreras^{1*}, Claudia Patricia Ruiz-Díaz², Marcos A. Quiñones-Otero³, and
4 Carlos Toledo-Hernández^{2*}

5 1- Department of Biology, University of Puerto Rico, Mayagüez campus, Call Box 9000,
6 Mayagüez, Puerto Rico 00681-9000

7 2- Sociedad Ambiente Marino; PO Box 22158, San Juan, Puerto Rico 00931-2158

8 3- University of Puerto Rico, Río Piedras campus, Planning Department, 10 Ave. Universidad,
9 Suite 1001, San Juan, Puerto Rico 00925-2530

10 **Corresponding authors:** ruber.rodriguez@upr.edu; carlostoledo@sampr.org

11 **Keywords:** *Diadema antillarum*, mass mortality, sea urchin, demography, Puerto Rico

12 **Abstract:**

13 Pervasive epizootic events have had a significant impact on marine invertebrates throughout the
14 Caribbean, leading to severe population declines and consequential ecological implications. One
15 such event was the regional collapse of herbivory, partly caused by the *Diadema antillarum*
16 mortality event in 1983-84, resulting in a trophic cascade and altering the structure of reef
17 communities. Consequently, there was a notable decrease in coral recruitment and an increase in
18 the coverage of macroalgae. Nearly four decades later, in early 2022, the Caribbean basin
19 experienced another widespread mass mortality event, further reducing the populations of *D.*
20 *antillarum*. To assess the effects of this recent mortality event on the current demographics of *D.*
21 *antillarum*, we surveyed eight populations along the eastern, northeastern, northern, and
22 northwestern coast of Puerto Rico from May to July 2022, estimating their population density,
23 size distribution, and disease prevalence. Additionally, the study compared these population
24 parameters with data from four sites previously surveyed in 2012 and 2017 to understand the
25 impact of the recent mortality event. The survey conducted in 2022 showed varying population
26 densities at the surveyed reefs. Some populations exhibited mean densities of nearly one
27 individual per square meter, while others had extremely low or no living individuals per square
28 meter. The four populations with the highest density showed no evidence of disease, whereas the
29 four populations with the lowest *D. antillarum* densities exhibited moderate to high disease
30 prevalence. However, when considering all sites, the estimated disease prevalence remained
31 below 5%. Nevertheless, the comparison with data from 2012 and 2017 indicated that the recent
32 mortality event had a negative impact on *D. antillarum* demographics at multiple sites, as the
33 densities in 2022 were reduced by 60.19% compared to those from the previous years. However,
34 it is still too early to determine the severity of this new mortality event compared to the 1983-84
35 mortality event. Therefore, it is imperative to continue monitoring these populations.

36 **Introduction**

37 Over recent years, the incidence of infectious diseases affecting marine organisms has increased
38 and resulted in structural and functional impacts on ecosystems (Yadak and Upadhyay 2023).
39 Even though infectious diseases are common in the marine realm, mass mortalities caused by
40 infectious diseases are rare, yet their effects can be dramatic and long-lasting. Mass mortalities
41 could be particularly damaging in regions characterized by a low redundancy of functional
42 groups, such as the Caribbean reefs (Carpenter 1990; Mumby *et al.*, 2006). Such events could
43 lead to a functional extinction of a key species (i.e., the level at which the species no longer
44 fulfills its ecological role) (Valiente *et al.*, 2015), compromising the community assemblage of
45 the entire region and consequently restructuring the services these ecosystems provide to
46 humankind and their ecological roles in the oceans (Lessios 1988; Carpenter 1990).

47 The prevalence of disease outbreaks is increasingly impacting the marine environment (Harvell
48 *et al.*, 1999). Reports of large-scale episodic events leading to mass mortalities in marine
49 organisms have increased since the latter half of the previous century (Hayes *et al.*, 2001).
50 Consequently, documented instances of population crash due to disease outbreak episodes have
51 been reported in many marine taxa. However, population crashes are not uncommon among
52 echinoderms (Hewson *et al.*, 2019; Lawrence 2020). This phylum is commonly referred to as a
53 "boom-bust" group due to the frequent outbreak episodes and massive die-offs observed
54 worldwide (Uthicke *et al.*, 2009). Echinoderms play an important ecological role in the
55 Caribbean region, not only as key herbivores, and structuring agents of the benthic community
56 (Sammarco 1982), but also due to their history of population crashes (Hughes *et al.*, 1985;
57 Steneck 2013).

58 Several mass-mortality events affecting coral reefs in the Caribbean have been recorded, but the
59 1980 *Diadema antillarum* mass mortality event has been the most serious and well-studied of all
60 (Lessios 2016). Before the die-off, *D. antillarum* was among the main herbivores native to
61 Caribbean coral reefs (Steneck 2013; Mercado-Molina *et al.*, 2015; Rodríguez-Barreras *et al.*,
62 2014). However, a mysterious waterborne pathogen(s) demised over 98% of the *D. antillarum*
63 population throughout the Caribbean basin (Lessios *et al.*, 1984; Hughes *et al.*, 1985).
64 Immediately after, and in subsequent decades, reef-building corals declined, while the coral reefs
65 experienced a significant increase in macroalgae, contributing to a severe decline in coral cover
66 (Lessios 2016). Nearly 40 years after the mass-mortality event, *D. antillarum* has shown variable
67 levels of recovery across the region; however, *D. antillarum* densities have not reached pre-
68 mortality levels in most localities (Mercado-Molina *et al.*, 2015; Rodríguez-Barreras *et al.*,
69 2015a; Pusack *et al.*, 2022).

70 In early 2022, a new mortality event of *D. antillarum* was reported on several islands across the
71 Caribbean (Response Network, AGRRA 2022). The mortality was first reported in the U.S.
72 Virgin Islands, and subsequently, mortalities were reported in several reefs throughout the
73 Caribbean. Many individuals have been found dead or showing signs of disease, i.e., sea urchins
74 outside their shelters in midday hours, unable to attach to the substrate, showing slow movement
75 of spines as a response to contact, and loss of spines (Hylkema *et al.*, 2023). It is known that the
76 species has a diurnal sheltering and nocturnal foraging behavior (Sharp *et al.*, 2023). The
77 resurgence of the *D. antillarum* die-off at a time when populations across the Caribbean have not
78 fully recovered is of great concern for the scientific community, given the poor ecological state

79 of Caribbean coral reefs (Levitin *et al.*, 2023). Monitoring demographic changes in keystone
80 species populations is essential for gaining insights into the biological relationships within an
81 ecosystem. Therefore, in this study, we surveyed *D. antillarum* populations along the eastern,
82 northern, and northwestern coasts of Puerto Rico. At each site, we estimated the population
83 density, size distribution, and disease prevalence. We subsequently compared these parameters to
84 available demographic data collected in 2012 and 2017 for four of these sites. These surveys
85 were driven by three central questions: 1) Is the disease found in all the surveyed reefs? 2) Is the
86 disease prevalence similar in all the surveyed reefs, and therefore are these reefs affected by the
87 disease in a similar way, and 3) Are different sizes of *D. antillarum* individuals equally affected
88 by the disease?

89 Materials and Methods

90 Surveyed sites

91 Surveys were carried out in eight shallow water reefs (< 3.0 m depth) along the eastern,
92 northeastern, northern, and northwestern coasts of Puerto Rico (**Figure 1**). These sites were
93 selected based on 1) the availability of demographic data from 2012 and 2017, and 2) divers who
94 posted images of diseased and dead *D. antillarum* individuals on social media. The surveys
95 started in May 2022, in Playa Punta Bandera located in Luquillo, on the northeastern coast
96 (**PBA**), and Cerro Gordo in Vega Baja (**CGO**), on the northern coast of Puerto Rico. Surveys
97 continued in June, 2022 when we visited Punta Tamarindo (**PTA**) and Punta Melones (**PME**),
98 both on Culebra Island, on the eastern coast of Puerto Rico; Playa Sardinera in Dorado, on the
99 northern coast (**PSA**), and Shacks Beach (**SBE**) and Playa Peña Blanca (**PBL**) in Aguadilla, both
100 on the northwestern coast of Puerto Rico. Surveys ended in July 2022, when we visited Playa El
101 Escambrón in San Juan on the northern coast (**ESC**) (**Table 1**).

102 PBA is a shallow bordering reef (< 2 m in depth), with coral cover ranging from 20-60% and
103 dominated by standing dead and live *Acropora palmata* and *Pseudodiploria strigosa* at the reef
104 crest. At the back reef, the substrate is dominated by *P. clivosa*, and *Porites furcata* mixed with
105 patches of *Thalassia testudinum* and *Syringodium filiforme*. Water clarity is nearly 10 m year-
106 round. CGO is a patchy reef interconnected with patches of seagrass beds dominated by *T.*
107 *testudinum* and, to a lesser extent, by *S. filiforme*. This reef is influenced by a natural freshwater
108 channel that drains nearly 100 m west of this reef. Coral cover at this reef is < 10%, and is
109 mainly dominated by *P. astreoides*, *P. strigosa*, and *P. clivosa*. Water clarity is highly variable,
110 ranging from < 2 m during the rainy season to > 10 m in the dry season. PTA and PME are
111 basaltic rock outcrops with coral coverage ranging from 15-20% dominated by massive coral
112 heads such as *Porites astreoides*, *Pseudodiploria strigosa*, *P. clivosa*, *Favia fragum*, and
113 standing dead *Acropora palmata*. Water clarity exceeds 10 m year-round. Data collected from
114 these reefs were compared with historical data available in Rodriguez-Barreras *et al.* (2018).

115 PSA is a shallow (< 1 m water depth) emergent aeolianite platform of 4.4 km², bordered by
116 seagrass beds dominated by *S. filiforme* and to a lesser extent *T. testudinum* and sand. Coral
117 cover is nearly 8% and is dominated by *Madracis mirabilis*, *P. furcata*, and *Siderastrea radians*.
118 Water clarity is highly variable, ranging from < 1 m during the rainy season to > 15 m in the dry
119 season. SBE is dominated by dead coral heads of *Orbicella* and *Acropora*, mixed with *P.*
120 *strigosa*, *P. clivosa*, and *A. palmata* at the reef crest and by *P. astreoides* and *A. palmata* and

121 octocorals the back reef. In this zone, coral coverage is < 5%. Water quality ranged between 3-
122 10m most of the year. PBL is a karstic in origin flat substrate, with a coral cover < 10%,
123 dominated by *Pseudodiploria strigosa*, *P. clivosa*, *P. labyrinthiformis*, *Porites astreoides* and
124 octocorals. Water clarity is > 8-10 m year-round. ESC is a submerged seawall of basaltic rocks
125 and steel girders oriented perpendicular to the shore. Coral coverage at this reef is less than 5%
126 and is dominated by *P. astreoides* and octocorals such as *Gorgonia ventalina*. The natural
127 substratum next to the rocks is a mixed assemblage of macroalgae and sand with small size
128 patches of *T. testudinum* and *S. filiforme*. Water clarity ranged between 1-5 meters year-round.

129 *Population parameters*

130 To determine sea urchin density, test diameter, and to be able to compare recently collected data
131 with the historical data, we followed Mercado-Molina *et al.* (2015) and Rodríguez-Barreras *et al.*
132 (2018). Briefly, at each reef and at hours ranging from 10:00 - 13:00, we set eight belt transects
133 of 20 m² (10 m x 2 m) parallel to the coast. Transects were at least 5 meters apart from each
134 other at depths ranging from 1-3 m, as at these depths sea urchin abundance tends to be higher
135 (Ruiz-Ramos *et al.*, 2011; Rodríguez-Barreras *et al.*, 2014; Mercado-Molina *et al.* 2015). We
136 counted all individuals within each transect, including the healthy, the diseased, and the dead
137 individuals. Sea urchin individuals were diagnosed as diseased if they were observed outside
138 their cavities in daylight hours, unable to attach to the substrate, showing slow movement of
139 spines as a response to contact and/or autotomy, i.e., loss of spines. We also carefully inspected
140 crevices between corals and small holes within each transect to avoid missing cryptic
141 individuals. These data were used to estimate the urchin density (i.e., the number of urchins per
142 transect per site). We also measured the test diameter of individuals collected from the transects
143 to estimate the size distribution at each reef. The total measured individuals per reef was 50.
144 When needed, sea urchins out of the transects were measured until reaching 50 individuals per
145 reef. Likewise, we also measured the tests from dead and sick sea urchins when possible. These
146 data were used to classify sea urchins into three size classes: small or juvenile (test diameter \leq
147 4.0 cm), medium or young adult (test diameter between 4.01 and 6.0 cm), and large or adult (test
148 diameter $>$ 6.01 cm) individuals. This data was used to construct a size-frequency distribution
149 (Miller *et al.*, 2003; Lugo-Ascorbe 2004; Rodríguez-Barreras *et al.*, 2014). Sampling was
150 approved by the Department of Natural and Environmental Resources of Puerto Rico, permit
151 number DRNA- 2022-IC-046.

152 *Data analysis*

153 We ran a general linear model with a Poisson distribution using the number of observations per
154 transect as the response variable and the surveyed reefs as the explanatory variable to determine
155 statistical differences between the 2022 sea urchin densities and between sites. To determine
156 statistical significances between the historical density (i.e., 2012 and 2017) and density data from
157 2022, we ran a general linear model with a Poisson distribution using the number of observed *D.*
158 *antillarum* individuals per transect as the response variable and reefs (CGO, PTA, PME, and
159 PBA) and years (i.e., 2012, 2017 and 2022) as the explanatory variables. To compare size
160 distribution based on the horizontal test diameter of *D. antillarum* among reefs during 2022, we
161 used a two-way ANOVA, with the test size (in cm) as the response variable and size categories
162 (small, medium, and large), and surveyed reefs as the explanatory variables. To determine
163 potential differences in size structure from data collected in 2012, 2017, and 2022, we ran a

164 three-way ANOVA using the test diameter (in cm) as the response variable and size categories
165 (small, medium, and large), surveyed reefs (CGO, PTA, PME, and PBA) and years (2012, 2017
166 and 2022) as the explanatory variables, and a Tukey post-hoc pairwise comparison. All statistical
167 analyses were conducted using R Statistical Software (v 4.3.1; R Core Team, 2023).

168 Results

169 Spatio-temporal abundance

170 Out of the eight sites visited from May to July 2022, seven had living *D. antillarum* (i.e., PBA,
171 CGO, PSA, SBE, PME, PBL, and ESC). We only observed dead individuals at PTA. Overall, a
172 total of 665 living *D. antillarum* individuals were counted, resulting in a local mean density of
173 $0.52 \pm 0.33 \text{ ind.m}^{-2}$ (mean \pm SD). The highest densities were observed in CGO (1.09 ± 0.26
174 ind.m^{-2}) and PBA ($1.05 \pm 0.89 \text{ ind.m}^{-2}$), followed by PSA and PBL with $0.79 \pm 0.43 \text{ ind.m}^{-2}$ and
175 $0.78 \pm 0.42 \text{ ind.m}^{-2}$, respectively. The lowest densities were found at PSA, ESC, and PME with
176 0.36 ± 0.27 , 0.11 ± 0.17 , and $0.01 \pm 0.02 \text{ ind.m}^{-2}$, respectively (**Figures 2 & 3**). The statistical
177 analysis revealed significant differences in mean densities among all sites except between PBA
178 and CGO (**Table S1**).

179 *D. antillarum* densities were highly variable from 2012, 2017, and 2022. Nonetheless, a
180 consistent pattern of increasing from 2012 to 2017 and decreasing between 2017 to 2022 was
181 observed at most of the surveyed reefs (**Figure 3**). For instance, at CGO, density increased by
182 4.03% from 2012 to 2017, but from 2017 to 2022, it decreased by 29.84%. At PBA, density
183 increased by 21.78% from 2012 to 2017 but decreased by 20.23% from 2017 to 2022 (**Figure 3**).
184 Likewise, at PTA, density increased by 6.30% from 2012 to 2017, yet no living individuals were
185 observed in 2022. In contrast, density at PME steadily declined across the survey. For instance,
186 from 2012 to 2017, density declined by 29%, and from 2017 to 2022 declined by 99%. Statistical
187 differences were found among sites between 2012 and 2017 with 2022, and the interaction
188 between sites and years (**Table 2S**).

189 Test diameter distribution

190 Overall, the mean diameter of *D. antillarum* tests across reefs in 2022 were relatively similar.
191 The highest test diameter was observed in PBA with $7.19 \pm 0.89 \text{ cm}$, followed by SBE with 7.03
192 $\pm 1.33 \text{ cm}$, PSA with $6.81 \pm 1.09 \text{ cm}$, ESC with $6.86 \pm 1.23 \text{ cm}$, CGO with $6.46 \pm 0.91 \text{ cm}$, and
193 PBL with $5.84 \pm 1.11 \text{ cm}$ (**Figure 4**). Only three individuals were measured at PME; the mean
194 test diameter was $5.11 \pm 1.07 \text{ cm}$. Similar test diameters were also recorded in 2012 and 2017.
195 For instance, in 2012, PTA exhibited the highest mean test diameter at $6.82 \pm 0.74 \text{ cm}$, followed
196 by PME and PBA with $6.78 \pm 0.77 \text{ cm}$ and $6.75 \pm 0.88 \text{ cm}$ respectively, and lastly, CGO with
197 $6.31 \pm 1.31 \text{ cm}$. In 2017, CGO showed the highest test diameter with $6.79 \pm 1.05 \text{ cm}$, followed
198 by PBA and PME with $6.60 \pm 1.13 \text{ cm}$ and $6.57 \pm 1.10 \text{ cm}$, respectively, and lastly, PTA with
199 $5.92 \text{ cm} \pm 0.96 \text{ cm}$ (**Figure 5**). Statistical differences were detected between reefs ($F= 5.334$ $df=$
200 3, $p\text{-value}= 0.001$), years ($F= 6.095$, $df= 2$, $p\text{-value}= 0.002$), and the interaction between sites and
201 years ($F= 6.75$, $df= 5$, $p\text{-value}= 4.23 \text{ e-}06$). The post-hoc analysis revealed differences between
202 PTA and the rest of the reefs across all years. The analysis also revealed differences between
203 PBA-2022 and PME-2017, PBA-2017 and PTA-2017, PBA-2022, and CGO-2022.

204 The 2022 test size distribution was dominated by individuals from the large size class
205 (individuals with tests > 6.01 cm) in most reefs (**Figure 4**). For instance, at PBA, 98% of the
206 encountered individuals belong to the adult size class and only 2% to the small size class. At
207 SBE, the large size class comprised 80% of the population, while the medium and small size
208 classes represented 18% and 2%, respectively. Meanwhile, at CGO, PSA, and ESC, the large
209 size class comprised between 70 to 76% of the population. Medium size class at ESC comprised
210 30%, while at PSA and CGO, the medium size class comprised 22 and 28 %. The small size
211 class individuals at CGO and PSA comprised around 2%. A similar demographic pattern was
212 observed in the populations surveyed in 2012 (**Figure 5**). For instance, the individuals from
213 larger size class comprised between 80-88% of *D. antillarum* populations at PBA, CGO, PME,
214 and PTA, whereas the medium size class ($4.0 < x \leq 6.01$ cm) comprised between 12 to 20%. No
215 small individuals (≤ 4.0 cm) were observed in 2012 at the surveyed sites, except in CGO (**Figure**
216 **5**). However, by 2017 we observed a decrease in the larger individuals, i.e., 86 to 50%, coupled
217 with an increase in the medium size class, 10 to 50%, and the smaller size class, e.g., 2 to 8%.
218 The statistical analysis showed differences by reefs, with CGO showing statistical differences
219 with PME and PTA. In addition, the analysis revealed significant differences by year, with 2012
220 being statistically different from 2022, and by size class categories, with the frequency of large
221 individuals being different from medium and small individuals (**Table 2**).

222 *Disease prevalence*

223 Of the total of 665 sea urchins counted from May to July of 2022, only 4.3% were diseased.
224 Diseased sea urchins were exclusively observed in DBE, PME, PTA, and ESC, but disease
225 prevalence varied among sites. For instance, disease prevalence at DBE and ESC was 11.02%
226 and 41.17%, respectively. Meanwhile, the observed individuals at the Culebra sites were either
227 diseased, as in the case of PME where two out of the three observed individuals were diseased,
228 or, as in the case of PTA, there were no live individuals. In addition, among the diseased sea
229 urchins, 92.6% of them belonged to the large size class, while the remaining 7% were accounted
230 for medium size class. No small diseased individuals were observed during the surveys at any of
231 the sites (**Figure 6**).

232 **Discussion**

233 *D. antillarum Density*

234
235 This study, conducted during the midst of the disease outbreak caused by *Scuticociliatosis*
236 (Hewson *et al.*, 2023), focuses on assessing the current density and size distribution of *D.*
237 *antillarum* in eight reefs located along the eastern, northeastern, northern, and northwestern
238 coasts of Puerto Rico. Furthermore, to determine the impact of this die-off, the study compares
239 the demographic parameters observed in 2022 with historical data. Our results indicate that the
240 disease impact on *D. antillarum* populations was heterogeneous across all surveyed sites, with
241 variations observed among different locations. However, all the observed diseased sea urchins
242 exhibited external signs of illness similar to those described in the literature by Hylkema *et al.*
243 (2023). Furthermore, the concurrent timing of our observations with those reported in other
244 Caribbean jurisdictions strongly suggests that we were indeed dealing with the same disease.

245 Our data reveals significant variability in the estimated densities of *D. antillarum* across the
246 surveyed reefs, with notable differences observed among sites. Of particular concern is the
247 considerable decrease in density in 2022 compared to historical data for the Culebra sites. This
248 reduction is significant considering that these sites had the highest densities on the eastern coast
249 of Puerto Rico in the early 2000s (Ruiz-Ramos et al. 2011). For instance, these authors reported
250 mean densities of $1.59 \pm 0.50 \text{ ind}\cdot\text{m}^{-2}$ at PTA, whereas no living individuals were detected in
251 2022. We also documented similar density at PME, where density dropped from 1.04 ± 0.90
252 $\text{ind}\cdot\text{m}^{-2}$ in 2017 to no healthy sea urchins detected in 2022. Other sites have experienced similar
253 *D. antillarum* reductions. For instance, Rodriguez-Barreras et al. (2014) reported densities of
254 $1.10 \text{ ind}\cdot\text{m}^{-2}$ at ESC, yet our 2022 survey revealed a density drop to $0.1 \text{ ind}\cdot\text{m}^{-2}$, with nearly half
255 of the individuals being affected by the disease. Given the current disease prevalence observed at
256 ESC, it is anticipated that the outbreak will have a more significant impact if the diseased
257 individuals do not recover, and the disease continues to spread. The other sites exhibited less
258 severe outbreak impact. For instance, PSA and PBL exhibited similar densities, but PSA
259 displayed a disease prevalence of over 10%, while no diseased individuals were detected in PBL.
260 Therefore, the density at PSA would likely have been higher than that of PBL if it had not been
261 affected by the outbreak event.

262 Densities at PBA and CGO have also experienced decreases even though evidence of disease
263 was not found. For instance, a study conducted in 2017 by Rodriguez-Barreras et al. (2018)
264 estimated the density at PBA at $1.26 \text{ ind}\cdot\text{m}^{-2}$, while the estimated current density decreased to
265 $1.05 \text{ ind}\cdot\text{m}^{-2}$. A similar declining trend was observed in CGO, where densities decreased from
266 $1.55 \text{ ind}\cdot\text{m}^{-2}$ in 2017 to $1.09 \text{ ind}\cdot\text{m}^{-2}$ in 2022, respectively. In subsequent visits to these sites in
267 February, May, and August 2023, we found no evidence of the disease, further suggesting that
268 the disease may not be the primary cause of these declines (unpublished data). Instead, habitat
269 degradation may have influenced the observed declines as multiple coral heads, including the
270 dominant species in this area e.g., *Pseudodiploria* spp., were either recently dead or exhibited
271 signs of Stony Coral Tissue Loss Disease (Dahlgren et al., 2021). Alternatively, the absence of
272 diseased or dead sea urchins among the studied reefs may result in some populations being more
273 resistant to the disease than others. It is also noteworthy to mention that from 2017 to 2022, three
274 hurricanes onslaught Puerto Rico. These hurricanes caused significant damage to the reefs and
275 seagrass beds, which, when combined with natural low recruitment, may have resulted in the
276 observed low density in 2022 when compared to the 2017 densities (Miller et al., 2009;
277 Rodriguez-Barreras et al., 2015a & 2015b; Pilnick et al., 2021).

278 *Size distribution*

279
280 The current size distribution of *D. antillarum* in the surveyed reefs was dominated by the large-
281 size class individuals, with fewer medium-sized class individuals and even fewer small-size class
282 individuals. The absence of juveniles may have multiple explanations. For instance, lower
283 frequencies of small-size individuals may suggest a generally low recruitment given the
284 relatively low abundance of mature and, therefore, larger *D. antillarum* individuals when
285 compared to 80s pre-mortality events. In fact, most authors argued this as the main reason for the
286 slow recovery after the massive mortality (Lessios 1988; Miller et al., 2003; Rodriguez-Barreras
287 et al., 2018). It could also suggest a high mortality among the recently settled and juvenile sea
288 urchins due to predation, as several studies have argued that *D. antillarum* predation by reef-

289 fishes may have a profound effect on the sea urchin size structure (Harbone *et al.*, 2009;
290 Rodriguez-Barreras *et al.*, 2015a). Nonetheless, it is difficult to conclude that the reason for the
291 low observations of juveniles and sub-adults was related to being more susceptible to the disease
292 than mature individuals. Therefore, longitudinal studies, which include a collection of *D.*
293 *antillarum* in the larval pool and recruit monitoring across several reefs, are required to better
294 comprehend the demographic dynamics of *D. antillarum* under the current outbreak scenario.
295

296 *Outbreak Impact*

297

298 Overall, the prevalence of the new outbreak was still relatively low in the surveyed reefs, as only
299 4.3 % of the 665 counted sea urchins were diseased (**Figure 6**). It also shows an erratic
300 geographic distribution, with some reefs showing high prevalence and others with moderately to
301 low prevalence and hence presumably low impact. A recent study conducted in the Dominican
302 Republic also reported variable impact across different reefs, although the outbreak in the
303 Dominican Republic seems to have had a higher impact than in Puerto Rico (Villalpando *et al.*,
304 2022). Nonetheless, the outbreak in Puerto Rico just started, as judged by the lack of conclusive
305 evidence of disease in some of the surveyed reefs. Therefore, it is still premature to capture the
306 real magnitude of the impact, and if the ongoing outbreak is as destructive as the 80s mortality
307 event when populations were decimated throughout the western Atlantic, including the
308 Bermudas, in a relatively short period of time (Mumby *et al.*, 2006; Bove *et al.*, 2022). Instead,
309 the spatial-heterogeneous nature of this new outbreak and the variable mortality of individuals
310 resemble the mortality event occurring in the sibling urchin species *D. africanum*, from October
311 2009 to April 2010 in the subtropical eastern Atlantic (Clemente *et al.*, 2014). Nonetheless, long-
312 term monitoring programs at these reefs may help disclose size class patterns of disease
313 susceptibility.

314

315 **Conclusion**

316 Populations of *D. antillarum* at surveyed reefs have not fully recovered since the mass
317 mortality event in the 1980s (Mercado-Molina *et al.*, 2015; Rodríguez-Barreras *et. al.*, 2018) and
318 are now facing a second outbreak that is causing further damage. This study sheds light on the
319 current state of *D. antillarum* populations in Puerto Rico's reefs amid the *Scutico ciliatosis*
320 outbreak, revealing different degrees of impact across different locations, with some reefs
321 experiencing a drastic decline in sea urchin density, particularly concerning for sites like
322 Culebra, which once boasted relative high densities. Nonetheless, the limited available data
323 makes it difficult to determine which factors (abiotic and biotic) may favor the infection either
324 by compromising the individual's immune system or by favoring the proliferation of the biotic
325 agent(s) or both. This 2022 outbreak's complexity mirrors past events, emphasizing the
326 importance of establishing long-term monitoring programs where key abiotic and biotic
327 components known to cause stress to other coral reefs-associated organisms are regularly
328 surveyed. This is especially critical in the face of climate change and changing marine
329 conditions, which may weaken the immunity of marine organisms and increase the frequency
330 and severity of disease outbreaks.

331

332 **Acknowledgments**

333

334 We want to express our gratitude to the Sociedad Ambiente Marino for providing logistic
335 support. We also want to thank Dr. Alberto Sabat and Dr. Benjamin Van Ee for their valuable
336 comments and corrections which helped us improve the manuscript's quality.

337

338 References

339 AGRRA. (2022). Diadema Response Network Map of Diadema and other sea urchins in the
340 Caribbean. www.agrra.org. ArcGIS Online.

341 Bove, C. B., Mudge, L., & Bruno, J. F. (2022). A century of warming on Caribbean reefs. *PLOS
342 Climate*, 1(3), e0000002.

343 Carpenter, R. C. (1990). Mass mortality of *Diadema antillarum*. *Marine Biology*, 104(1), 67-77.

344 Clemente, S., Lorenzo-Morales, J., Mendoza, J. C., López, C., Sangil, C., Alves, F., ... &
345 Hernández, J. C. (2014). Sea urchin *Diadema africanum* mass mortality in the subtropical
346 eastern Atlantic: role of waterborne bacteria in a warming ocean. *Marine Ecology Progress Series
347 Series*, 506, 1-14.

348 Dahlgren, C., Pizarro, V., Sherman, K., Greene, W., & Oliver, J. (2021). Spatial and temporal
349 patterns of stony coral tissue loss disease outbreaks in the Bahamas. *Frontiers in Marine
350 Science*, 8, 682114.

351 Harvell, C. D., Kim, K., Burkholder, J. M., Colwell, R. R., Epstein, P. R., Grimes, D. J., ... &
352 Vasta, G. R. (1999). Emerging marine diseases--climate links and anthropogenic
353 factors. *Science*, 285(5433), 1505-1510.

354 Hayes, M. L., Bonaventura, J., Mitchell, T. P., Prospero, J. M., Shinn, E. A., Van Dolah, F., &
355 Barber, R. T. (2001). How are climate and marine biological outbreaks functionally linked? *The
356 Ecology and Etiology of Newly Emerging Marine Diseases*, 213-220.

357 Hewson, I., Sullivan, B., Jackson, E. W., Xu, Q., Long, H., Lin, C., ... & Sewell, M. A. (2019).
358 Perspective: something old, something new? Review of wasting and other mortality in
359 Asteroidea (Echinodermata). *Frontiers in Marine Science*, 406.

360 Hewson, I., Ritchie, I. T., Evans, J. S., Altera, A., Behringer, D., Bowman, E., ... & Breitbart, M.
361 (2023). A scuticociliate causes mass mortality of *Diadema antillarum* in the Caribbean
362 Sea. *Science Advances*, 9(16), eadg3200.

363 Hylkema, A., Kitson-Walters, K., Kramer, P. R., Patterson, J. T., Roth, L., Sevier, M. L., ... &
364 Lang, J. C. (2023). The 2022 *Diadema antillarum* die-off event: Comparisons with the 1983-
365 1984 mass mortality. *Frontiers in Marine Science*, 9, 2654.

366 Hughes, T. P., Keller, B. D., Jackson, J. B. C., & Boyle, M. J. (1985). Mass mortality of the
367 echinoid *Diadema antillarum* Philippi in Jamaica. *Bulletin of Marine Science*, 36(2), 377-384.

368 Karlson, R. H., & Levitan, D. R. (1990). Recruitment-limitation in open populations of *Diadema
369 antillarum*: an evaluation. *Oecologia*, 82, 40-44.

370 Lawrence, J. M. (2020). Mass mortality of echinoderms from abiotic factors. In *Echinoderm studies 5 (1996)* (pp. 103-137). CRC Press.

372 Lessios, H. A. (1988). Mass mortality of *Diadema antillarum* in the Caribbean: what have we learned? *Annual review of ecology and systematics*, 371-393.

374 Lessios, H. A. (2016). The great *Diadema antillarum* die-off: 30 years later. *Annu. Rev. Mar. Sci.* 8, 267-283. doi: 10.1146/annurev-marine-122414-033857

376 Lessios, H. A., Cubit, J. D., Robertson, D. R., Shulman, M. J., Parker, M. R., Garrity, S. D., & 377 Levings, S. C. (1984). Mass mortality of *Diadema antillarum* on the Caribbean coast of 378 Panama. *Coral Reefs*, 3(4), 173-182.

379 Levitan, D. R., Best, R. M., & Edmunds, P. J. (2023). Sea urchin mass mortalities 40 y apart 380 further threaten Caribbean coral reefs. *Proceedings of the National Academy of Sciences*, 381 120(10), e2218901120.

382 Lugo-Ascorbe, M. A. (2004). Population status of the black sea urchin *Diadema antillarum* 383 (Philippi) in La Parguera, Puerto Rico, 20 years after the mass mortality event (Doctoral 384 dissertation).

385 Mercado-Molina, A. E., Montañez-Acuña, A., Rodríguez-Barreras, R., Colón-Miranda, R., Díaz- 386 Ortega, G., Martínez-González, N., ... & Sabat, A. M. (2015). Revisiting the population status of 387 the sea urchin *Diadema antillarum* in northern Puerto Rico. *Journal of the Marine Biological 388 Association of the United Kingdom*, 95(5), 1017-1024.

389 Miller, R. J., Adams, A. J., Ogden, N. B., Ogden, J. C., & Ebersole, J. P. (2003). *Diadema 390 antillarum* 17 years after mass mortality: is recovery beginning on St. Croix? *Coral Reefs*, 22(2), 391 181-187.

392 Miller, M. W., Kramer, K. L., Williams, S. M., Johnston, L., & Szmant, A. M. (2009). 393 Assessment of current rates of *Diadema antillarum* larval settlement. *Coral Reefs*, 28, 511-515.

394 Mumby, P. J., Hedley, J. D., Zychaluk, K., Harborne, A. R., & Blackwell, P. G. (2006). 395 Revisiting the catastrophic die-off of the urchin *Diadema antillarum* on Caribbean coral reefs: 396 fresh insights on resilience from a simulation model. *Ecological modelling*, 196(1-2), 131-148.

397 Pilnick, A. R., O'Neil, K. L., Moe, M., & Patterson, J. T. (2021). A novel system for intensive 398 *Diadema antillarum* propagation as a step towards population enhancement. *Scientific Reports*, 399 11(1), 11244.

400 Pusack, T. J., Stallings, C. D., Albins, M. A., Benkwitt, C. E., Ingeman, K. E., Kindinger, T. L., 401 & Hixon, M. A. (2022). Protracted recovery of long-spined urchin (*Diadema antillarum*) in the 402 Bahamas. *Coral Reefs*, 1-6.

403 R Core Team (2023). R: A language and environment for statistical computing. R Foundation for 404 Statistical Computing, Vienna, Austria. URL <https://www.R-project.org/>.

405 Rodríguez-Barreras, R., Pérez, M. E., Mercado-Molina, A. E., Williams, S. M., & Sabat, A. M.
406 (2014). Higher population densities of the sea urchin *Diadema antillarum* linked to wave
407 sheltered areas in north Puerto Rico Archipelago. *Journal of the Marine Biological Association
408 of the United Kingdom*, 94(8), 1661-1669.

409 Rodríguez-Barreras, R., Pérez, M. E., Mercado-Molina, A. E., & Sabat, A. M. (2015a). Arrested
410 recovery of *Diadema antillarum* population: survival or recruitment limitation? *Estuarine,
411 Coastal and Shelf Science*, 163, 167-174.

412 Rodríguez-Barreras, R., Durán, A., Lopéz-Morell, J., & Sabat, A. M. (2015b). Effect of fish
413 removal on the abundance and size structure of the sea urchin *Diadema antillarum*: a field
414 experiment. *Marine Biology Research*, 11(10), 1100-1107.

415 Rodríguez-Barreras, R., Montanez-Acuna, A., Otano-Cruz, A., & Ling, S. D. (2018). Apparent
416 stability of a low-density *Diadema antillarum* regime for Puerto Rican coral reefs. *ICES Journal
417 of Marine Science*, 75(6), 2193-2201.

418 Ruiz-Ramos, D. V., Hernández-Delgado, E. A., & Schizas, N. V. (2011). Population status of the
419 long-spined urchin *Diadema antillarum* in Puerto Rico 20 years after a mass mortality event.
420 *Bulletin of Marine Science*, 87(1), 113-127.

421 Sammarco, P. W. (1982). Polyp bail-out: an escape response to environmental stress and a new
422 means of reproduction in corals. *Marine ecology progress series*. *Oldendorf*, 10(1), 57-65.

423 Sharp, W. C., Delgado, G. A., Pilnick, A. R., & Patterson, J. T. (2023). Diurnal sheltering
424 behavior of hatchery-propagated long-spined urchins (*Diadema antillarum*): a re-examination
425 following husbandry refinements. *Bulletin of Marine Science*, 99(2), 97-108.

426 Steneck, R. S. (2013). Sea urchins as drivers of shallow benthic marine community structure.
427 In *Developments in Aquaculture and Fisheries Science* (Vol. 38, pp. 195-212). Elsevier.

428 Tuohy, E., Wade, C., & Weil, E. (2020). Lack of recovery of the long-spined sea urchin
429 *Diadema antillarum* Philippi in Puerto Rico 30 years after the Caribbean-wide mass mortality.
430 *PeerJ*, 8, e8428.

431 Uthicke, S., Schaffelke, B., & Byrne, M. (2009). A boom–bust phylum? Ecological and
432 evolutionary consequences of density variations in echinoderms. *Ecological monographs*, 79(1),
433 3-24.

434 Valiente-Banuet, A., Aizen, M. A., Alcántara, J. M., Arroyo, J., Cocucci, A., Galetti, M., ... &
435 Zamora, R. (2015). Beyond species loss: the extinction of ecological interactions in a changing
436 world. *Functional Ecology*, 29(3), 299-307.

437 Yadav, N., & Upadhyay, R. K. (2023). Global Effect of Climate Change on Seasonal Cycles,
438 Vector Population and Rising Challenges of Communicable Diseases: A Review. *Journal of
439 Atmospheric Science Research| Volume*, 6(01).

440

Table 1(on next page)

Table 1

Surveyed sites along the eastern and northern coasts of Puerto Rico and Culebra Islands.

1 **Table 1.** Surveyed sites along the eastern and northern coasts of Puerto Rico and Culebra Islands.

Site	Acronym	County	Lat.	Long.	Coral cover (%)	Depth (m)
Punta Tamarindo	PTA	Culebra	18.3151	-65.3179	15 - 20	1 - 2
Punta Melones	PME	Culebra	18.3041	-65.3112	15 - 20	1 - 3
El Escambron	ESC	San Juan	18.4660	-66.0858	< 5	0.5 - 3
Punta Bandera	PBA	Luquillo	18.3882	-65.7185	15 - 20	0.5 - 1
Cerro Gordo	CGO	Vega Alta	18.4850	-66.3389	< 10	1 - 3
Shacks Beach	SBE	Isabela	18.5164	-67.1001	< 5	1 - 3
Peña Blanca	PBL	Aguadilla	18.4724	-67.1691	< 10	1 - 3
Playa Sardinera	PSA	Dorado	18.4768	-66.2984	< 5	0.5 - 1

Table 2(on next page)

Table 2

A post-hoc pairwise Tukey test comparison of horizontal test diameter among sites of Puerto Rico Island. Sites with no living Diadema [Punta Tamarindo (PTA) and Punta Melones (PME)] were excluded from the analysis. Sites are Punta Bandera (PBA), El Escambrón (ESC), Cerro Gordo (CGO), Playa Sardinera (PSA), Shacks Beach (SBE), and Playa Peña Blanca (PBL). The red color indicates a significant difference.

1 **Table 2.** A post-hoc pairwise Tukey test comparison of horizontal test diameter among sites of
2 Puerto Rico Island. Sites with no living Diadema [Punta Tamarindo (PTA) and Punta Melones
3 (PME)] were excluded from the analysis. Sites are Punta Bandera (PBA), El Escambrón (ESC),
4 Cerro Gordo (CGO), Playa Sardinera (PSA), Shacks Beach (SBE), and Playa Peña Blanca (PBL).
5 The red color indicates a significant difference.

6

7

8	Sites	CGO	PBA	DBE	PBL	SBE	ESC
9	CGO		0.000	0.054	0.050	0.001	0.110
10	PBA			0.083	0.000	0.714	0.243
11	PSA				0.000	0.171	0.885
12	PBL					0.000	0.002
13	SBE						0.373
14	ESC						

13

14

15

16

17

Figure 1

Figure 1. Surveyed sites along the eastern and northern coasts of Puerto Rico and Culebra Islands.

Punta Tamarindo (PTA) and Punta Melones (PME) in Culebra Island, Punta Bandera (PBA), El Escambrón (ESC), Cerro Gordo (CGO), Playa Sardinera (PSA), Shacks Beach (SBE), and Playa Peña Blanca (PBL). Image credit: Open Street Map. Esri World Imaginary

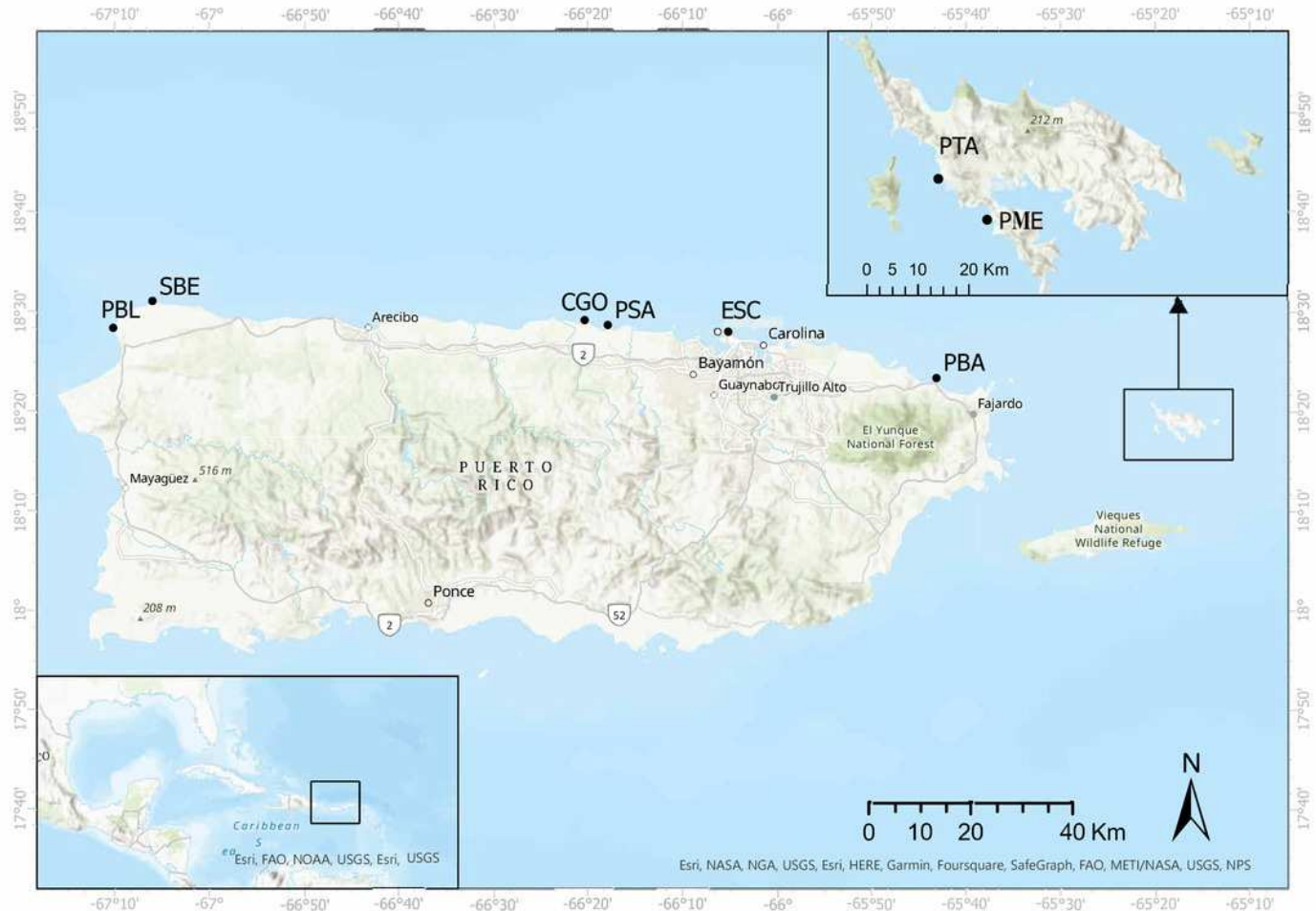


Figure 2

Figure 2. Boxplot showing the 2022 *Diadema antillarum* abundance across Cerro Gordo (CGO), El Escambrón (ESC), Punta Bandera (PBA), Playa Peña Blanca (PBL), Punta Melones (PME), Playa Sardinera (PSA), Punta Tamarindo (PTA), Shacks Beach (SBE).

The red circle represents the mean, the median is represented by the bold line, the extremes of the boxplot are the 1st and 3rd quartiles, and the whiskers are the maximum and minimum. The black dots represent the outliers.

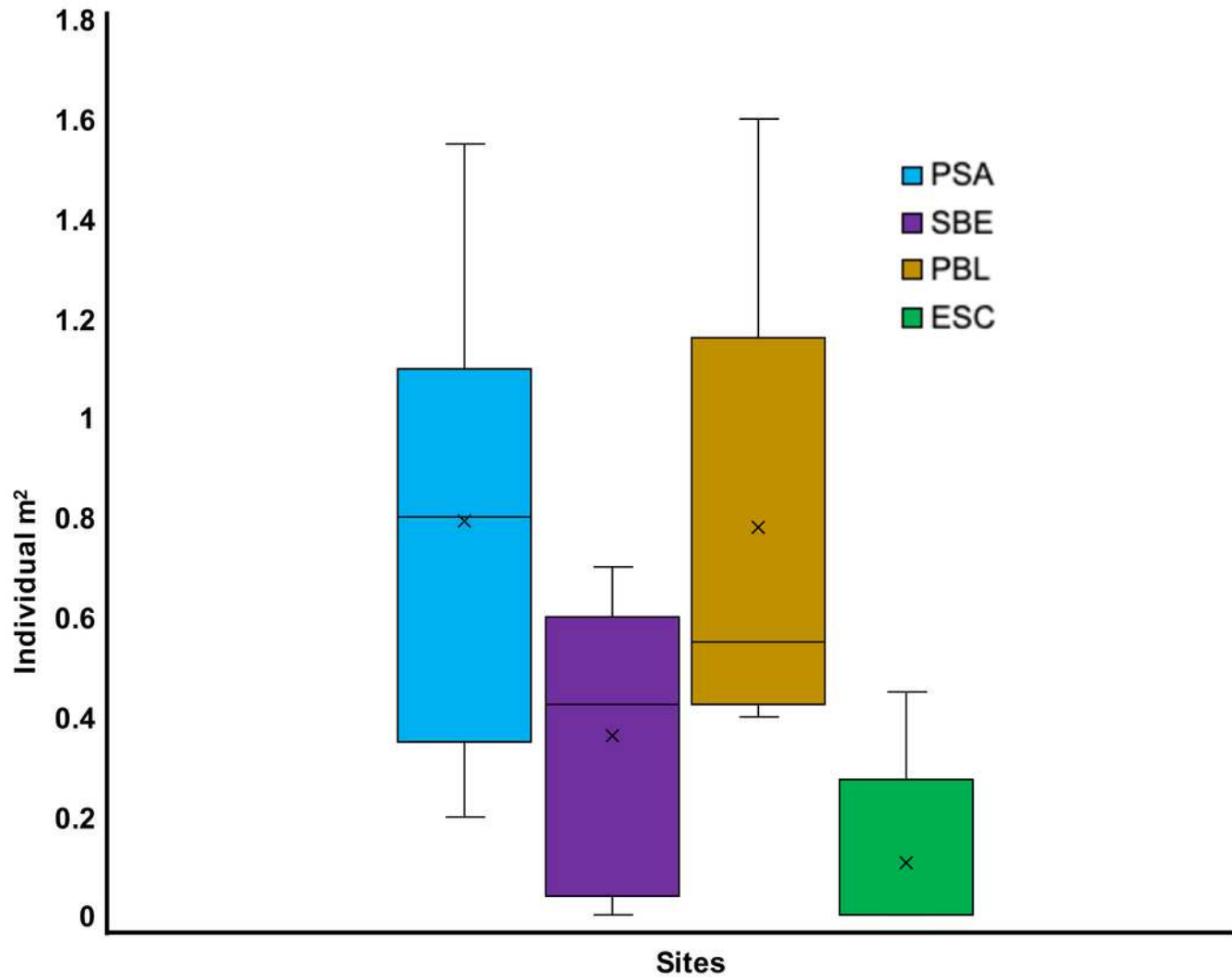


Figure 3

Figure 3. Boxplot showing the *Diadema antillarum* density across years 2012, 2017 & 2022 at (A) Cerro Gordo (CGO), (B) Punta Bandera (PBA), (C) Punta Tamarindo (PTA), and (D) Punta Melones (PME).

In the Boxplot, the yellow circle represents the mean, the median is presented by the bold line, the extreme of the Boxplot are the 1st and 3rd quartiles, and the whiskers are the maximum and minimum.

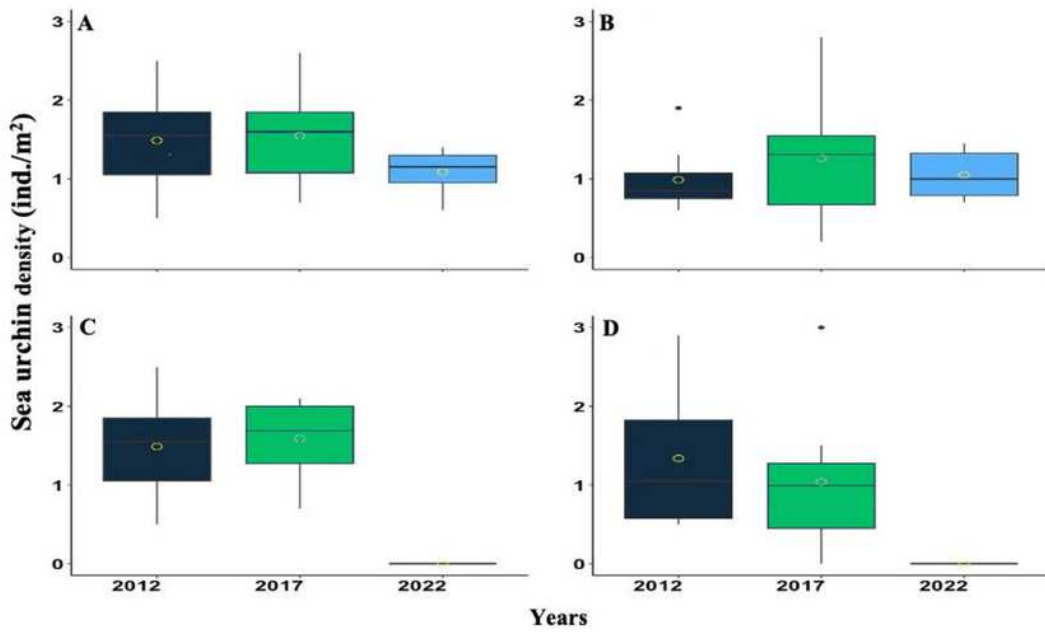


Figure 4

Figure 4. Boxplot showing the test diameter of *Diadema antillarum* in 2022 across the study sites (A) and by Size Categories (B).

Sites are Cerro Gordo (CGO), Escambrón (ESC), Punta Bandera (PBA), Playa Peña Blanca (PBL), Punta Melones (PME), Playa Sardinera (PSA), and Shacks Beach (SBE). Size class category: small (≤ 4.0 cm), medium (4.01 to 6.01 cm), and large (> 6.01 cm). In the Boxplot, the red circle represents the mean, the median is presented by the bold line, the extreme of the Boxplot are the 1st and 3rd quartiles, and the whiskers are the maximum and minimum.

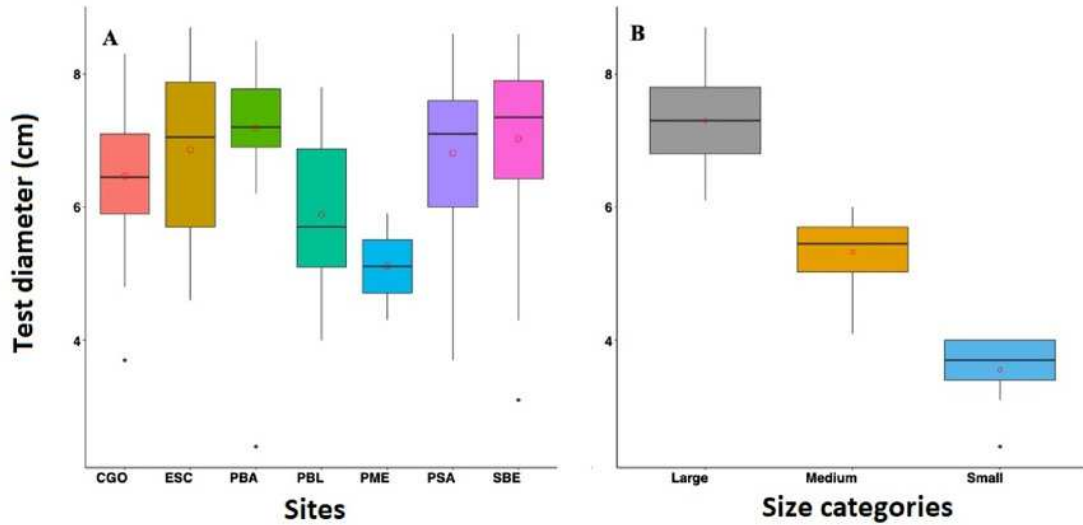


Figure 5

Figure 5. Size categories distribution across years 2012, 2017 and 2022 at four sites, where A is Cerro Gordo (CGO), B is Punta Bandera (PBA), C Punta Melones (PME), and D is Punta Tamarindo (PTA).

Size class category: small (≤ 4.0 cm), medium (4.01 to 6.0 cm), and large (> 6.01 cm).

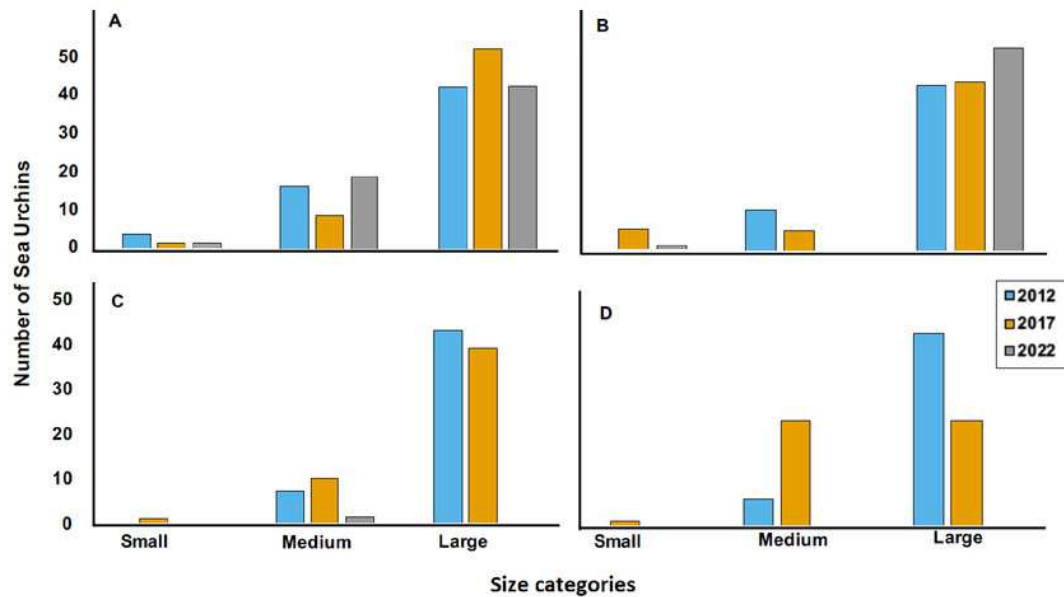


Figure 6

Figure 6. Overall disease sea urchin size class distribution in Puerto Rico for the eight surveyed sites in 2022.

Notice that no small diseased individuals were observed. In the Boxplot, the red circle represents the mean, the median is presented by the bold line, the extreme of the Boxplot are the 1st and 3rd quartiles, and the whiskers are the maximum and minimum.

